

Long-lived spin echoes in a magnetically dilute system: An NMR study of Ge single crystals

A. M. Panich,^{1,*} N. A. Sergeev,² and I. Shlimak³

¹*Department of Physics, Ben-Gurion University of the Negev, P.O. Box 653, Beer Sheva 84105, Israel*

²*Institute of Physics, University of Szczecin, 70-451 Szczecin, Poland*

³*Jack and Pearl Resnick Institute of Advanced Technology, Physics Department, Bar-Ilan University, Ramat Gan 52900, Israel*

(Received 22 March 2007; revised manuscript received 1 August 2007; published 1 October 2007)

Owing to the well-developed technology, isotopic engineering of Si and Ge semiconductors permits one to control the density of nuclear spins and vary the spin coherence time, a crucial parameter in spintronics and quantum computing where nuclear spin is used as a qubit. In the present paper, we report on the NMR study of ^{73}Ge nuclear spin decoherence in germanium single crystals with different abundances of the ^{73}Ge isotope. Our measurements of Hahn- and solid-echo decays show that they are well fit by a superposition of two exponentials; at that, the deviation from the single exponential is more pronounced in the more spin-diluted sample, causing long-lived echoes. We show that the decay of these echoes becomes slower with the reduction of ^{73}Ge abundance and is therefore caused by dipole-dipole interaction, reflecting the fundamental decoherence process in the spin system. The fast decay at the beginning of the relaxation process is shown to be mainly caused by the quadrupole interaction. Our experimental findings are supported by the calculations of Hahn- and solid-echo decays in the germanium crystals under study. Quite good agreement between the theory and experiment is demonstrated.

DOI: [10.1103/PhysRevB.76.155201](https://doi.org/10.1103/PhysRevB.76.155201)

PACS number(s): 03.67.Lx, 71.20.Nr, 76.60.-k, 82.56.-b

I. INTRODUCTION

Semiconductor-based architectures are quite realistic in constructing the large-scale quantum computer (QC) owing to the well-developed semiconductor technology. Among the QC concepts under discussion, nuclear spins are considered to be the ideal quantum bits (qubits) embodied in semiconductor crystals, particularly in Si and Ge. The choice of Si and Ge is determined by the fact that in both these crystals, only one isotope (^{29}Si among three stable Si isotopes and ^{73}Ge among five stable Ge isotopes) has nuclear spin and therefore isotopic engineering of Si and Ge permits one to control the density of nuclear spins and vary the spin coherence time, a crucial parameter in spintronics and quantum computing where nuclear spin is used as a qubit. Therefore, a number of nuclear magnetic resonance (NMR) studies have been carried out in order to investigate the nuclear spin decoherence in silicon.¹⁻⁴ Demytyev *et al.*¹ and Watanabe and Sasaki,² who measured NMR in the Si powders with the natural abundance of ^{29}Si isotope, have brought an unusual result, showing different characters of the decoherence processes after applying the Hahn-echo sequence, on the one hand, and Carr-Purcell and Carr-Purcell-Meiboom-Gill (CPMG) pulse sequences, on the other hand. While the Hahn-echo sequence yielded single exponential decay with the time constant $T_2=5.6$ ms, the CPMG sequence resulted in a double-exponential decoherence process, which time constants were evaluated as 15 and 200 ms.² Since all silicon atoms in the cubic Si structure are equivalent, the origin of the observed biexponential decay is unclear. One of the reasons for such a behavior may be the appearance of stimulated echo induced by the CPMG pulse train.⁵

Against the intensive NMR studies of silicon mentioned above, analogous investigation of germanium is absent, despite that the Ge crystals are considered as a promising material for spin-based quantum computers. In the present pa-

per, we report on the NMR study of ^{73}Ge nuclear spin decoherence in germanium single crystals with different abundances of the ^{73}Ge isotope. We show that accurate measurements of the Hahn- and solid-echo decay envelopes yield nonexponential echo decays and that the deviation from the single exponential is more pronounced in the more spin-diluted sample, producing long-lived echoes. We show that the decay of these echoes becomes slower with the reduction of ^{73}Ge abundance and is therefore caused by dipole-dipole interaction, reflecting the fundamental decoherence process in the spin system. The fast decay at the beginning of the relaxation process is shown to be mainly caused by the quadrupole interaction. Our experimental findings are supported by the calculations of Hahn- and solid-echo decays in the germanium crystals under study. Quite good agreement between the theory and experiment is demonstrated.

II. EXPERIMENTAL DETAILS

All experiments were performed on the single crystalline Ge samples with the ^{73}Ge abundance of $f=1\%$ and 7.76% (natural abundance), later denoted as Ge-1% and Ge-7.76% crystals, respectively. ^{73}Ge NMR spectra and spin-spin (T_2) and spin-lattice (T_1) relaxation times were measured in the external magnetic field $B_0=8.0196$ T (resonance frequency $\nu_0=11.908$ MHz) using a Tecmag pulse NMR spectrometer and an Oxford superconducting magnet. The ^{73}Ge NMR spectra were obtained using Fourier transformation of the free induction decays (FIDs) and Hahn⁶ and solid echoes.⁷ Spin-spin relaxation (decoherence) time T_2 was measured using both Hahn- and solid-echo pulse sequences, $(\pi/2)_0-\tau-(\pi)_{90}-\tau'$ -echo and $(\pi/2)_0-\tau-(\pi/2)_{90}-\tau'$ -echo, respectively. Here, the subscript indicates the relative phase of the carrier. In all echo measurements, we used 4- and 16-step phase cycling procedures in order to suppress residual FID signal and reduce pulse-coherent noise and ar-

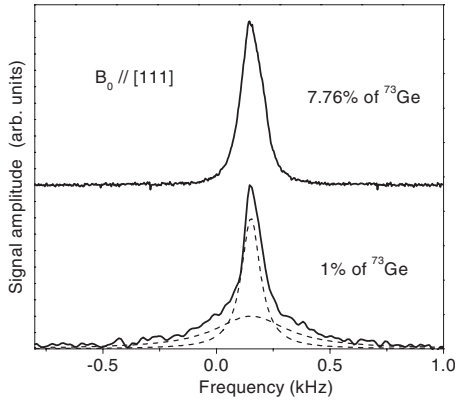


FIG. 1. Room temperature ^{73}Ge NMR spectra of the Ge-7.76% (top) and Ge-1% (bottom) single crystals. External magnetic field B_0 is applied along the [111] direction. Dashed lines show the bi-Lorentzian fit.

tifacts. ^{73}Ge spin-lattice relaxation time T_1 was measured by means of a saturation comb pulse sequence. All data were collected at the ambient temperature.

III. RESULTS OF THE EXPERIMENTS

^{73}Ge spectra of the germanium crystals with $f=1\%$ and 7.76%, measured in magnetic field B_0 applied along the [111] direction, are shown in Fig. 1. The spectra are symmetric resonances with the linewidth $\Delta\nu=110$ Hz. When $B_0\parallel[110]$, the linewidth is $\Delta\nu=88$ Hz. Dipolar contribution to the linewidth can be estimated using the Van Vleck formula.⁸ The diamondlike crystal structure of Ge yields the second moment values $S_2=877$ and 688 Hz^2 for $B_0\parallel[111]$ and $B_0\parallel[110]$, respectively. For Gaussian line shape, it would correspond to $\Delta\nu=70$ and 62 Hz, respectively. Magnetic field inhomogeneity of our spectrometer is evaluated to be around 3 ppm. We note that ^{73}Ge is a quadrupolar nucleus, having spin $I=9/2$ and nuclear quadrupole moment $q=-0.19$ b. Therefore, additional contribution to the linewidth comes from the quadrupole interaction of ^{73}Ge nuclei with small random electric field gradient, resulting from the crystal imperfections that cause small local deviations from cubic symmetry at the nucleus site. In a perfect crystal, similar contribution is shown to be induced by the isotopic disorder among germanium atoms.^{9,10} Both these effects result in the first-order quadrupolar broadening of the resonance line. From our experimental data and calculations of the quadrupolar effects,^{9,10} one can conclude that in germanium crystal with natural isotope abundance, the contributions to the NMR linewidth coming from the magnetic dipole-dipole interaction, quadrupole interaction, and magnetic field inhomogeneity are of the same order of magnitude. In the isotopically diluted Ge-1% crystal, the dipole-dipole coupling is significantly reduced. In spite of this fact, the NMR spectra of this crystal (Fig. 1) show broader wings in comparison with the Ge-7.76% crystal, which is evidently caused by the worse crystal perfection and larger contribution coming from the first-order quadrupole coupling.

Spin-lattice relaxation times were measured to be $T_1=12.2\pm 0.1$ and 11.6 ± 2.1 s for the Ge-7.76% and Ge-1%, respectively. These T_1 's are much shorter compared to those in silicon, whose T_1 is ~ 4 h at ambient temperature and of the order of tens to hundreds of hours in the ^{29}Si -enriched sample at liquid helium temperature.^{3,4} It is known that the nuclear spin-lattice relaxation in semiconductors is driven by several mechanisms. In the case of the nuclear spin $I=1/2$, the most important of them is the hyperfine interaction of nuclear spins with the spins of free carriers. At that, the relaxation rate is proportional to the free carrier density. Therefore, one can suggest that the faster spin-lattice relaxation in Ge, in comparison with that in Si, might be attributed to the larger free carrier density in germanium. (At $T=300$ K, intrinsic semiconductor Ge crystal exhibits a carrier concentration of 2.33×10^{13} cm^{-3} , while Si shows only 1.02×10^{10} cm^{-3}). However, since ^{73}Ge is a quadrupolar nucleus, it should exhibit an additional powerful relaxation mechanism due to the interaction of nuclear quadrupole moment with fluctuating (due to the lattice vibrations) electric field gradient. Verkhovskii *et al.*⁹ discussed this effect in germanium and showed that the quadrupolar relaxation is the primary relaxation mechanism. Spin-lattice relaxation assisted by nuclear dipole-dipole interaction would yield $T_1\sim 1/f$ dependence that was not observed in the experiment, allowing us to exclude this mechanism from the consideration.

While T_1 is the time at which the energy of the spin system is exchanged with the environment, spin-spin relaxation time T_2 is the time at which *information* is exchanged and which manifests as the loss of phase coherence. Thus, the T_2 scale is the important time scale for quantum computation. To measure the spin-spin relaxation (decoherence) time T_2 , both Hahn- and solid-echo pulse sequences with varying delay τ between pulses have been applied. It is known that the Hahn echo⁶ is formed by the interactions that are linear in the spin operators of the resonant nucleus and thus requires some inhomogeneity of the applied magnetic field. Echo maximum following the $(\pi/2)_0-\tau-(\pi)_{90}-\tau'$ -echo pulse sequence typically occurs near $\tau'=\tau$. At that, the Hahn-echo decay is caused by the interactions that are quadratic in the nuclear spin operators, such as dipolar and quadrupolar couplings, since the sign of these interactions is not changed by the π pulse. On the other hand, solid (or "quadrupolar") echo^{7,11} is formed by the interactions that are quadratic in the nuclear spin operators, i.e., by both dipolar and quadrupolar couplings, though the refocusing of these interactions by the solid-echo sequence is not complete. Decay of the solid echo is caused by a modified (due to the second rf pulse) Hamiltonian of the above interactions⁷ as well as by the inhomogeneity of the applied magnetic field. Since, as shown above, all aforementioned contributions are present in the germanium crystal and are of the same order of magnitude, both Hahn and solid echoes are formed in the crystals under study. At that, the echo maxima after the second pulse occur at $\tau'=\tau$, except for a very small deviation from this position at the short time domain. In the latter case, we use the term "echo decay envelope" to refer to the decay of the signal amplitude at the time τ' as a function of the total evolution time ($\tau'+\tau$).

The echo decay envelopes in the germanium crystal with the natural isotope abundance are given in Figs. 2 and 3 for

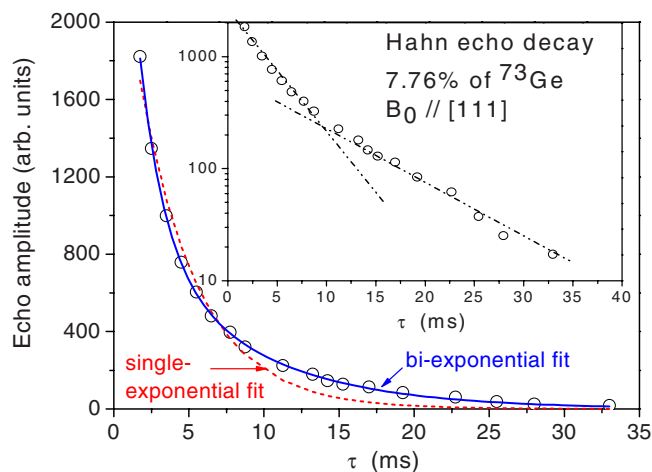


FIG. 2. (Color online) ^{73}Ge Hahn-echo decay envelope in the linear and semilogarithmic (insert) scales in Ge single crystal with natural abundance of ^{73}Ge isotope. External magnetic field is applied along the [111] axis. Dashed and solid lines show single and biexponential fits, respectively.

two crystal orientations regarding the applied magnetic field, namely, when B_0 is along the [111] and [110] axes. In both cases, we observe nonexponential Hahn- and solid-echo decays, which may be well fitted by a superposition of at least two exponentials,

$$M(t) = M_1(0)\exp(-2\pi t/T_{21}) + M_2(0)\exp(-2\pi t/T_{22}), \quad (1)$$

with $M_1(0)$, $M_2(0)$, T_{21} , and T_{22} as adjusting parameters. This is well seen from Figs. 2 and 3 that show the echo decay in the linear and semilogarithmic scales. Decay parameters T_{21} and T_{22} , obtained by fitting these plots, are given in Table I.

The observed effect is much more pronounced in measurements of the germanium crystal with 1% of ^{73}Ge . In this crystal, both Hahn- and solid-echo decay envelopes exhibit strikingly nonexponential behavior (Figs. 4 and 5). T_{21} and T_{22} values, obtained from the fit of these plots, are given in Table I.

We note that the statistical theory of NMR line shape^{12,13} in magnetically diluted systems with dipolar coupling among the spins predicts an exponential FID and Lorentzian line shape with the linewidth proportional to the nuclear spin concentration ($\Delta\nu \sim f$). In such a case, T_2 should be inversely

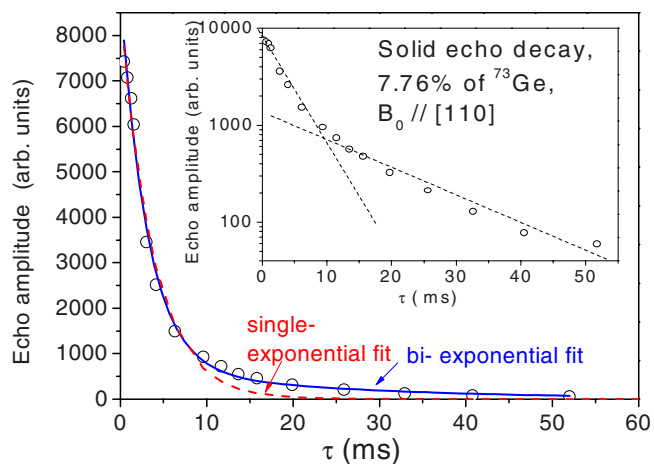


FIG. 3. (Color online) ^{73}Ge solid-echo decay envelope in the linear and semilogarithmic (insert) scales in Ge single crystal with natural abundance of the ^{73}Ge isotope. External magnetic field is applied along the [110] axis. Dashed and solid lines show single and biexponential fits, respectively.

proportional to the isotope content. One can find out from Table I that the experimentally measured decay of the echoes at the long-time domain, described by the time T_{22} , becomes slower with the reduced ^{73}Ge abundance, and the ratio $T_{22}(\text{Ge-1\%})/T_{22}(\text{Ge-7.76\%})$ is more or less close to the reciprocal ratio of the isotope contents. Therefore, we are led to the conclusion that the slow part of the decay is caused by the dipole-dipole interaction among nuclear spins and reflects the primary decoherence (dephasing) process in the spin system.

Let us now consider the origin of the fast echo decay at the beginning of the relaxation process. In our experiment (Table I), we observed that the decay time T_{21} of this process is shorter in the Ge-1% crystal in comparison with the Ge-7.76% crystal. It means that this effect is not caused by the dipole-dipole interaction. At that, the reduction in T_{21} in the crystal with 1% of ^{73}Ge correlates with the broader line wings observed in this crystal, which are caused by the quadrupole interaction. Therefore, we conclude that the initial part of the echo decay is mainly caused by the quadrupole interaction. Qualitatively, this effect may be described in the following manner. For nuclear spin $I=9/2$, the frequency of the central transition ($-\frac{1}{2} \leftrightarrow \frac{1}{2}$) is not shifted in the first order by the quadrupole interaction, while the frequencies of the

TABLE I. Experimental nuclear spin decoherence times T_{21} and T_{22} in Ge single crystals. Accuracy is around 10%–15%.

	T_{21} (ms) (Hahn echo)	T_{22} (ms) (Hahn echo)	T_{21} (ms) (solid echo)	T_{22} (ms) (solid echo)
Ge-7.76%, $B_0 \parallel [111]$	5.8	15.8	4.9	40
Ge-7.76%, $B_0 \parallel [110]$	7.1	17	7.2	36
Ge-1%, $B_0 \parallel [111]$	1.8	185	2	191
Ge-1%, $B_0 \parallel [110]$	1.75	127	1.9	201

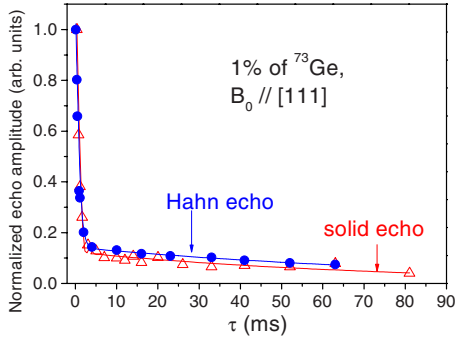


FIG. 4. (Color online) ^{73}Ge Hahn-echo and solid-echo decay envelopes in Ge single crystal with 1% of the ^{73}Ge isotope. External magnetic field is applied along the [111] axis. Thin solid lines show biexponential fits.

other transitions are shifted and the satellite lines corresponding to transitions $m \leftrightarrow (m-1)$ with $m \neq \frac{1}{2}$ appear on each side of the central line.¹² Since in our crystals the quadrupole interaction is not large, the latter transitions are not resolved and may be described by a broad envelope. At that, the central transition is broadened by dipole-dipole interactions only and therefore shows a narrow line. In the time domain, these two components would cause two different decays, i.e., fast decay caused by the quadrupole interaction and slow decay caused by the dipole-dipole interaction. Assuming that the aforementioned line shapes are Lorentzian, we would obtain a biexponential decay observed in the experiment with time constants T_{21} and T_{22} related to quadrupole and dipole couplings, respectively. This consideration seems to be correct at least for the Hahn echo. The above conclusion will be discussed in more detail and supported theoretically in the next section.

IV. THEORY

In order to support the above conclusions, we have carried out calculations of the Hahn- and solid-echo decays. The shape of the echo signal following a $(\pi/2)_0 - \tau - R - \tau' - \text{echo}$ pulse sequence is described by^{11,12}

$$E(\tau', \tau) = \frac{1}{\text{Tr}(I_X^2)} \text{Tr}(e^{-iH\tau'} R e^{-iH\tau} I_X e^{iH\tau} R^{-1} e^{iH\tau'} I_X), \quad (2)$$

where $\hbar H$ represents the secular terms of the spin Hamiltonian in the rotating frame and operator R describes the action of the second radio frequency pulse.

The interaction Hamiltonian of the ^{73}Ge nuclei (spin $I = 9/2$) can be written as

$$H = \sum_j H_j + \sum_{i < j} H_{ij}. \quad (3)$$

Here, H_j is the sum of the magnetic and quadrupolar energies of a nucleus j ,

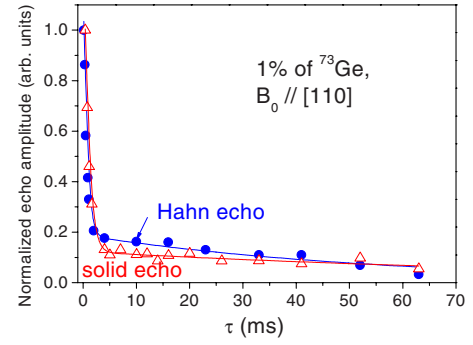


FIG. 5. (Color online) ^{73}Ge Hahn-echo and solid-echo decay envelopes in Ge single crystal with 1% of the ^{73}Ge isotope. External magnetic field is applied along the [110] axis. Thin solid lines show bi-exponential fits.

$$H_j = -\delta_j I_{Zj} + \omega_{Qj} \left[I_{Zj}^2 - \frac{1}{3} I(I+1) \right]. \quad (4)$$

The first term in Eq. (4) is the interaction of nuclear spin with inhomogeneous magnetic field within a sample. The quadrupole frequency ω_{Qj} is given by

$$\omega_{Qj} = \frac{3e^2 Q V_{ZZ}^{(j)}}{4I(2I-1)}. \quad (5)$$

The second term in Eq. (3) is the secular part of the magnetic dipole-dipole interaction between the nuclear spins i and j ,

$$H_{ij} = b_{ij} \left[I_{Zi} I_{Zj} - \frac{1}{4} (I_{+i} I_{-j} + I_{-i} I_{+j}) \right], \quad (6)$$

where

$$b_{ij} = \hbar \gamma^2 (1 - 3 \cos^2 \theta_{ij}) / r_{ij}^3, \quad (7)$$

\vec{r}_{ij} is the vector connecting the i th and j th spins, and θ_{ij} is the angle between \vec{r}_{ij} and applied magnetic field \vec{B}_0 .

As shown by Sergeev *et al.*,^{14,15} the expression [Eq. (2)] can be written in the form

$$E(\tau', \tau) = \sum_{k,n} a_{nk} G_k(\tau') G_n(\tau), \quad (8)$$

where

$$a_{nk} = \frac{\langle k | R n R^{-1} \rangle}{\langle 0 | 0 \rangle}. \quad (9)$$

The inner product in Eq. (9) is defined as

$$\langle k | n \rangle = \text{Tr}(k^+ n). \quad (10)$$

The vectors $|k\rangle$ satisfy the recurrence relation

$$|k\rangle = L|k-1\rangle - \nu_{k-2}^2 |k-2\rangle, \quad (11)$$

where

$$\nu_k^2 = \frac{\langle k+1 | k+1 \rangle}{\langle k | k \rangle}, \quad (12)$$

and $L = [H, \dots]$ is the Liouville superoperator. The functions $G_k(t)$ in Eq. (8) satisfy the system of the connected equations

TABLE II. Parameters Δ_d , Δ , and Δ_Q (in Hz) calculated from the experimental data (Table I) using Eqs. (15) and (16).

Isotope content	Method	$B_{0\parallel}[111]$			$B_{0\parallel}[110]$		
		Δ_Q	Δ_d	$\Delta_d+\Delta$	Δ_Q	Δ_d	$\Delta_d+\Delta$
Ge-7.76%	Hahn echo	34	63		28	59	
Ge-7.76%	Solid echo	37		83	14		93
Ge-1%	Hahn echo	111	5.4		114	7.8	
Ge-1%	Solid echo	148		17.6	156		16.7

$$i\dot{G}_0(t) = \nu_0^2 G_1(t),$$

...

$$i\dot{G}_k(t) = G_{k-1}(t) + \nu_k^2 G_{k+1}(t), \quad (13)$$

where the function $G_0(t)$ is the FID, which appears after the single 90° pulse.

We note that the ^{73}Ge nuclei are randomly distributed over the sites of the magnetically diluted germanium crystal lattice, yielding the random distributions of the coupling constants δ_j , ω_{Qj} , and b_{ij} . Suggesting these distributions to be Lorentzian, we calculated (Appendixes A and B) the Hahn-echo and solid-echo decay envelopes as

$$E(2\tau) \approx 0.85 \exp(-2\tau/T_{21}) + 0.15 \exp(-2\tau/T_{22}), \quad (14)$$

where

$$T_{21} = \frac{1}{5\Delta_Q}, \quad T_{22} = \frac{1}{\Delta_d} \quad (15)$$

for the Hahn echo and

$$T_{21} = \frac{1}{3.25\Delta_Q + \Delta_d + \Delta}, \quad T_{22} = \frac{1}{0.3(\Delta_d + \Delta)} \quad (16)$$

for the solid echo. Here, Δ_Q , Δ_d , and Δ are the half widths at the half height of the Lorentzian distributions of the quadrupole (ω_{Qj}) and dipole-dipole (b_{ij}) interaction constants in the spin-diluted sample and distribution of the magnetic field inhomogeneity (δ_j), respectively.

V. DISCUSSION

The expressions for the T_{12} 's and T_{22} 's derived in the previous section reflect the realistic physical picture of the spin-spin relaxation that was depicted above in Sec. III. First, these expressions show that the Hahn- and solid-echo decays may be described by a superposition of two exponentials, which is in agreement with the biexponential ^{73}Ge decays observed in the experiment. Second, theory shows that the rapidly relaxing component of the Hahn echo is caused by the quadrupole interaction, while the decay of the slowly relaxing component is caused by the dipole-dipole coupling, as expected according to the physical fundamentals. Third, for solid echo, the fast decay is caused by a combination of the quadrupole interaction, dipole-dipole interaction, and

magnetic field inhomogeneity, while the slowly decaying part is caused by the dipole-dipole coupling and magnetic field inhomogeneity, which also follows from the physical fundamentals. These findings explain the observed difference in Hahn- and solid-echo decays as well.

Assuming that the statistical theory of NMR line shape^{12,13} in magnetically diluted systems, predicting the linewidth to be proportional to the nuclear spin concentration, is the case, one is led to the conclusion that T_{22} should be inversely proportional to the isotope content. Such tendency was observed in the experiment.

Shortening of T_{12} in the Ge-1% crystal in comparison with that in the crystal with the natural abundance of the ^{73}Ge isotope is explained by the worse perfection of the former, which correlates with the broader wings observed in this crystal (Fig. 1).

Let us now use the experimental data on T_{12} and T_{22} (Table I) in order to calculate parameters Δ_d , Δ , and Δ_Q by means of Eqs. (15) and (16). The results of these calculations are given in Table II. One can find that the calculated dipolar linewidth in the crystal with 7.76% of ^{73}Ge is of the same order of magnitude that expected from Van Vleck's formula⁸ (Sec. III). The calculated quadrupolar parameter Δ_Q is close to that estimated as half width of the broader Lorentzian (Fig. 1) describing the first-order quadrupole broadening. This contribution is larger in the Ge-1% crystal in comparison with that in the Ge-7.76% crystal owing to the worse perfection of the former, as it was mentioned above. The evaluated magnetic field inhomogeneity is comparable to that produced by our magnet, though the formula of T_{22} in Eq. (16) yields the understated estimate of Δ in the case of the Ge-1% crystal. Nevertheless, one can conclude that our calculations yield reasonable values of Δ_d , Δ , and Δ_Q , demonstrating that the theory gives quite satisfactory description of the echo decays, in spite of the approximate character of computations. The first approximation in our calculation is the neglect of the flip-flop term in the Hamiltonian [Eq. (A2)], though the condition $|b_{ij}| \ll |\delta_j - \delta_i|$, yielding Eq. (A2), is hardly realized in the Ge-7.76% crystal. The second is the replacement of Eqs. (A5) and (B7) by the approximate expressions [Eqs. (A8) and (B8)], respectively. Also, we restricted our calculations taking into account the first terms of the series Eq. (8) only.

Let us now discuss the eventual application of Ge as a material for quantum computers, in which ^{73}Ge nuclear spins are used as qubits. One of the main goals in quantum computing is the elongation of decoherence time T_2 . To do this, one should prepare spin-diluted crystals in order to reduce

dipole-dipole interactions, which were found to be responsible for the slow echo decay. Nowadays, well-developed semiconductor technology allows successful isotopic engineering and growing the pure monoisotopic ^{70}Ge crystal enriched up to the level of 99.99%, which means that the content of the ^{73}Ge isotope is less than 0.01%.¹⁶ Assuming that spin decoherence is mainly dominated by dipole-dipole interactions, our findings show that in such a crystal, decoherence time T_2 would be elongated up to ~ 20 s. At that, we neglected the other limiting factors, such as the contribution of the second-order quadrupole interaction to T_2 of the central transition, thermal fluctuations of quadrupole interactions due to phonons, relaxation by hyperfine couplings to thermally excited carriers, etc. While a detailed evaluation of those contributions is out of the scope of our paper, the upper limit for decoherence time is actually fixed by the spin-lattice relaxation time $T_1 \sim 12$ s. This mechanism is not ^{73}Ge spin concentration dependent and would become dominant for highly spin-diluted samples; at that, the quadrupolar contribution to T_1 will be reduced in more perfect crystals. Anyhow, the decoherence time of ~ 12 s is quite an encouraging result for the application of this material in SiGe structures, which are suggested in different proposals for the experimental realization of nuclear spin-based quantum computers.¹⁷⁻¹⁹

VI. SUMMARY

In summary, our ^{73}Ge NMR measurements of Hahn- and solid-echo decay envelopes in germanium single crystals with different abundances of the ^{73}Ge isotope show that the echo decay is caused by two different decoherence processes. The fast decay at the beginning of the relaxation process is mainly caused by the quadrupole interaction. Then, this process proceeds to slowly decaying, long-lived spin echoes that are caused by dipole-dipole interaction among nuclear spins. This slow decay may be elongated by means of spin dilution. Our experimental findings are supported by the calculations of Hahn- and solid-echo decays in the germanium crystals. The formulas for both decay parameters are derived. Using these formulas and the experimental values of T_2 's, the reasonable values of dipolar and quadrupolar couplings were calculated. The variations of these couplings correlate with the variations observed in the NMR spectra. Elongation of the slow component of the dephasing process with depletion of Ge crystal with the ^{73}Ge isotope is encouraging for the application of this material in SiGe structures for a nuclear spin-based quantum computer.

ACKNOWLEDGMENTS

We thank A. N. Ionov for providing us with the Ge-1% crystal. I.S. thanks the Erick and Sheila Samson Chair of Semiconductor Technology for financial support.

APPENDIX A: HAHN-ECHO DECAY IN Ge CRYSTAL

Since the dipolar term in the Hamiltonian [Eq. (3)] does not commute with the other terms, the contributions to the echo response [Eq. (2)] from different terms of the Hamil-

tonian cannot be separated, making the calculation of the echo decay in analytic form impossible. Therefore, in the present work, we use a simplified model neglecting the flip-flop terms of the dipolar Hamiltonian and using it in the form $H_{ij} = b_{ij} I_{Zi} I_{Zj}$, which is a quite good approach for magnetically diluted systems with $|b_{ij}| \ll |\delta_j - \delta_i|$ (Refs. 1, 3, and 12) and allows us to noticeably simplify calculation and to receive physically reasonable data. Using the above approximation, one can write

$$\exp(iHt) = \prod_j \exp(-i\delta_j\tau) \exp(i\omega_{Qj} I_{Zj}^2) \exp\left(iI_{Zj} \sum_i b_{ij} I_{Zi}\right) \quad (\text{A1})$$

and turn from the consideration of the spin dynamic of the system of ^{73}Ge nuclei to the consideration of the echo response from each ^{73}Ge nucleus j with the Hamiltonian

$$H_j = -\delta_j I_{Zj} + \omega_{Qj} \left[I_{Zj}^2 - \frac{1}{3} I(I+1) \right] + d_j I_{Zj}, \quad (\text{A2})$$

where

$$d_j = \sum_i b_{ij} I_{Zi}. \quad (\text{A3})$$

The final result will be averaged over the random distributions of coupling constants δ_j , ω_{Qj} , and d_j .

For the Hahn echo, the operator $R = \exp(-i\pi I_X)$. Using the Hamiltonian [Eq. (A2)], Eq. (8) from Sec. IV, and results of Sergeev *et al.*,^{14,15} we obtain

$$E(\tau', \tau) = \cos[\delta_j(\tau' - \tau)] G_0(\tau' + \tau). \quad (\text{A4})$$

Here, $G_0(t)$ is the shape of FID, described by the Hamiltonian [Eq. (A2)] with $\delta_j = 0$. It is easy to show that

$$G_0(t) = (1/165) \cos(d_j t) [18 \cos(8\omega_{Qj} t) + 32 \cos(6\omega_{Qj} t) + 42 \cos(4\omega_{Qj} t) + 48 \cos(2\omega_{Qj} t) + 25]. \quad (\text{A5})$$

Assuming the Lorentzian distribution of δ_j ,

$$f(\delta_j) = \frac{\Delta}{\pi} \frac{1}{\delta_j^2 + \Delta^2}, \quad (\text{A6})$$

where Δ is the half width at the half height, we have from Eq. (A4) that

$$\begin{aligned} E(\tau', \tau) &= G_0(\tau' + \tau) \int f(\delta_j) \cos[\delta_j(\tau' - \tau)] d\delta_j \\ &= \exp[-\Delta(\tau' - \tau)] G_0(\tau' + \tau). \end{aligned} \quad (\text{A7})$$

Simplification of Eq. (A5) yields an approximate expression

$$G_0(t) = \frac{25}{165} \cos(d_j t) + \frac{140}{165} \cos(b_{Qj} t). \quad (\text{A8})$$

The parameter b_{Qj} is found from the condition

$$M_2 = -\ddot{G}_0(t)|_{t=0} = d_j^2 + \frac{96}{5}\omega_{Qj}^2 = \frac{25}{165}d_j^2 + \frac{140}{165}b_{Qj}^2, \quad (\text{A9})$$

where M_2 is the second moment of the Fourier transformed FID signal. From Eq. (A9), it follows that $b_{Qj}^2 \approx 5\omega_{Qj}$. Inserting Eq. (A8) into Eq. (A7) and assuming that the distributions of d_j and ω_{Qj} can be described by the Lorentzian functions

$$f_d(d_j) = \frac{\Delta_d}{\pi} \frac{1}{d_j^2 + \Delta_d^2}, \quad f_Q(\omega_{Qj}) = \frac{\Delta_Q}{\pi} \frac{1}{\omega_{Qj}^2 + \Delta_Q^2}, \quad (\text{A10})$$

we obtain for the echo amplitude ($\tau' = \tau$),

$$E(2\tau) \approx 0.85 \exp(-2\tau/T_{21}) + 0.15 \exp(-2\tau/T_{22}), \quad (\text{A11})$$

where

$$T_{21} = \frac{1}{5\Delta_Q}, \quad T_{22} = \frac{1}{\Delta_d}. \quad (\text{A12})$$

APPENDIX B: SOLID ECHO DECAY IN Ge CRYSTAL

For the solid echo, $R = \exp[-i(\pi/2)I_X]$. Using the Hamiltonian [Eq. (A2)], one obtains

$$E(\tau', \tau) = \exp[-\Delta(\tau' + \tau)] \times [G_0(\tau' - \tau) + M_{4e}G_2(\tau')G_2(\tau) + \dots]. \quad (\text{B1})$$

Here, Δ describes the distribution of δ_j that is assumed to be Lorentzian,

$$M_{4e} = \frac{4\omega_{Qj}^4}{35} [-8I^2(I+1)^2 + 22I(I+1) - 12] - \frac{2\omega_{Qj}^2 d_j^2}{5} [4I(I+1) - 3]. \quad (\text{B2})$$

For nuclear spin $I=9/2$, Eq. (B2) leads to

$$M_{4e} = -\frac{192}{5}\omega_{Qj}^2(13\omega_{Qj}^2 + d^2). \quad (\text{B3})$$

Here, $G_0(t)$ is given by Eq. (A5). As it follows from Eq. (13), the function $G_2(t)$ is

$$G_2(t) = -\frac{M_2}{M_4 - M_2^2} \left[G_0(t) + \frac{1}{M_2} \ddot{G}_0(t) \right], \quad (\text{B4})$$

where M_2 and M_4 are the second and the fourth moments of the Fourier transformed FID signal,

$$M_2 = d_j^2 + \frac{96}{5}\omega_{Qj}^2, \quad M_4 = d_j^4 + 36\frac{16}{5}d_j^2\omega_{Qj}^2 + 3(16)^2\omega_{Qj}^4. \quad (\text{B5})$$

Using Eqs. (B3) and (B4) and assuming that $d_j/\omega_{Qj} < 1$ and that the distributions of ω_{Qj} and d_j are described by the Lorentzian functions, we obtain

$$\begin{aligned} 1 + M_{4e}G_2(\tau)G_2(\tau) &= 1 - 0.325 \exp(-2\Delta_d\tau) \\ &\quad - [1 + \exp(-2\Delta_d\tau)] \\ &\quad \times [0.385 \exp(-2\Delta_Q\tau) \\ &\quad - 0.035 \exp(-4\Delta_Q\tau) \\ &\quad - 0.335 \exp(-6\Delta_Q\tau) \\ &\quad - 0.385 \exp(-8\Delta_Q\tau) \\ &\quad - 0.22 \exp(-10\Delta_Q\tau) \\ &\quad + 0.01 \exp(-12\Delta_Q\tau) \\ &\quad - 0.145 \exp(-14\Delta_Q\tau) \\ &\quad + 0.11 \exp(-16\Delta_Q\tau)]. \end{aligned} \quad (\text{B6})$$

Insertion Eq. (B6) into Eq. (B1) brings the following expression for the solid-echo amplitude ($\tau' = \tau$):

$$\begin{aligned} E(2\tau) &= \exp(-2\Delta\tau) - 0.325 \exp[-2(\Delta_d + \Delta)\tau] \\ &\quad - \{\exp(-2\Delta\tau) + \exp[-2(\Delta_d + \Delta)\tau]\} \\ &\quad \times [0.385 \exp(-2\Delta_Q\tau) - 0.035 \exp(-4\Delta_Q\tau) \\ &\quad - 0.335 \exp(-6\Delta_Q\tau) - 0.385 \exp(-8\Delta_Q\tau) \\ &\quad - 0.22 \exp(-10\Delta_Q\tau) + 0.01 \exp(-12\Delta_Q\tau) \\ &\quad - 0.145 \exp(-14\Delta_Q\tau) + 0.11 \exp(-16\Delta_Q\tau)]. \end{aligned} \quad (\text{B7})$$

Simplification of Eq. (B7) yields an approximate expression

$$E(2\tau) \approx 0.85 \exp(-2\tau/T_{21}) + 0.15 \exp(-2\tau/T_{22}), \quad (\text{B8})$$

where

$$T_{21} = \frac{1}{3.25\Delta_Q + \Delta_d + \Delta}, \quad T_{22} = \frac{1}{0.3(\Delta_d + \Delta)}. \quad (\text{B9})$$

We note that for short times, the expressions [Eqs. (B7) and (B8)] coincide.

*Corresponding author: pan@bgu.ac.il

¹A. E. Dementyev, D. Li, K. MacLean, and S. E. Barrett, Phys. Rev. B **68**, 153302 (2003).

²S. Watanabe and S. Sasaki, Jpn. J. Appl. Phys., Part 2 **42**, L1350 (2003).

³T. D. Ladd, D. Maryenko, Y. Yamamoto, E. Abe, and K. M. Itoh, Phys. Rev. B **71**, 014401 (2005).

⁴A. S. Verhulst, I. G. Rau, Y. Yamamoto, and K. M. Itoh, Phys. Rev. B **71**, 235206 (2005).

⁵M. B. Franzoni and P. R. Levstein, Phys. Rev. B **72**, 235410

- (2005).
- ⁶E. Hahn, *Phys. Rev.* **80**, 580 (1950).
- ⁷J. G. Powles and J. H. Strange, *Proc. Phys. Soc. London* **82**, 6 (1963).
- ⁸J. H. Van Vleck, *Phys. Rev.* **74**, 1168 (1948).
- ⁹S. V. Verkhovskii, A. Ya. Yakubovsky, B. Z. Malkin, S. K. Saikin, M. Cardona, A. Trokiner, and V. I. Ozhogin, *Phys. Rev. B* **68**, 104201 (2003).
- ¹⁰S. V. Verkhovskii, A. Ya. Yakubovsky, A. Trokiner, B. Z. Malkin, S. K. Saikin, V. I. Ozhogin, A. V. Tikhomirov, A. V. Ananyev, A. P. Gerashenko, and Yu. V. Piskunov, *Appl. Magn. Reson.* **17**, 557 (1999).
- ¹¹P. Mansfield, *Phys. Rev.* **137**, A961 (1965).
- ¹²A. Abragam, *The Principles of Nuclear Magnetism* (Clarendon, Oxford, 1961).
- ¹³P. W. Anderson, in *Proceedings of the American Physical Society*, *Phys. Rev.* **82**, 291 (1951) (see p. 342).
- ¹⁴N. A. Sergeev, A. V. Sapiga, and D. S. Ryabushkin, *Phys. Lett. A* **137**, 210 (1989).
- ¹⁵N. A. Sergeev, *Solid State Nucl. Magn. Reson.* **10**, 45 (1997).
- ¹⁶A. V. Inyushkin, A. N. Taldenkov, V. I. Ozhogin, K. M. Itoh, and E. E. Haller, *Phys. Rev. B* **68**, 153203 (2003).
- ¹⁷B. E. Kane, *Fortschr. Phys.* **48**, 1023 (2000).
- ¹⁸I. Shlimak, V. I. Safarov, and I. D. Vagner, *J. Phys.: Condens. Matter* **13**, 6059 (2001).
- ¹⁹I. Shlimak and I. Vagner, *Phys. Rev. B* **75**, 045336 (2007).